Sensitivity Analysis for Takeoff and Landing Distance Parameters for Regional Air Mobility (RAM) Aircraft

Gabino Martinez Rodriguez* Nathaniel J. Blaesser,† and Nicholas K. Borer‡
NASA Langley Research Center, Hampton, VA 23681

Takeoff and landing performance models require low-speed aerodynamic and thrust characteristics that are difficult to predict in the conceptual design stage. Although an empirical approach can be utilized to predict takeoff and landing performance, this approach is inadequate for aircraft incorporating novel technologies and design such as those proposed for regional air mobility aircraft. The focus of this paper is to understand the sensitivity of takeoff and landing distance to aerodynamic, propulsive, and other parameters of interest for regional air mobility class vehicles. The aerodynamic and propulsive characteristics are generated and modified using simplified approximations based on fundamental physics and integrated into the equations of motion to calculate takeoff and landing distances. The most impactful parameters for takeoff and landing were those related to propulsion and the lift curve. Additional impactful parameters for landing included braking coefficient, approach angle, and wing incidence. Lesser impact was observed for the parameters describing the low-speed drag polar.

I. Nomenclature

C_D	=	Coefficient of drag
C_{D_0}	=	Zero-lift coefficient of drag
C_{Di}	=	Coefficient of induced drag
C_L	=	Three-dimensional coefficient of lift
$C_{L_{\max}}$	=	Maximum lift coefficient
C_{L_α}	=	Lift curve slope
ΔC_L	=	Delta lift coefficient
C_T	=	Coefficient of thrust
D	=	Propeller Diameter
J	=	Advance ratio
J_L	=	Advance ratio linear break point
k_1	=	Linear coefficient term in drag polar
k_2	=	Quadratic coefficient term in drag polar
n	=	Revolutions per second
P	=	Shaft power
T	=	Thrust
V	=	Velocity
α	=	Angle of attack
α_m	=	Maximum angle of attack
ρ	=	Freestream air density
η_p	=	Propeller efficiency

II. Introduction

Fixed wing aircraft have two primary wing sizing considerations in the conceptual design phase. The first, occurring in low-speed flight regimes, is the wing area required to generate enough lift to takeoff and land safely. The second is

*Aerospace Engineer, Aeronautics Systems Analysis Branch, 5 Langley Blvd, Hampton, VA, Member
†Deputy Lead - Aero Concepts Incubator, Aeronautics Systems Analysis Branch, 5 Langley Blvd, Hampton, VA, Senior Member
‡Lead - Aero Concepts Incubator, Aeronautics Systems Analysis Branch, 5 Langley Blvd, Hampton, VA, Associate Fellow

high-speed cruise, where energy economy and therefore drag is the primary concern. Within this trade space, low-speed performance tends to require a larger wing area than is needed for cruise. In order to ameliorate the disparity in wing size, aircraft designs may need to incorporate additional elements and technologies like traditional high-lift devices or distributed electric propulsion (DEP). Traditional high-lift devices, such as flaps or slats, increase the wing area and modify the wing lifting characteristics. The augmentation of lift generation improves the aircraft's takeoff and landing (TOL) performance with the caveat that the high-lift devices need to retract and fit into the wing. Another approach to high-lift systems is the utilization of DEP to blow the wing's leading edge at low speeds. The greater dynamic pressure augments the wing's lift generation compared to that from forward velocity alone, improving the aircraft's TOL performance. The improved TOL performance (regardless of the high-lift technology used) then allows the aircraft's wing to be sized primarily for cruise, improving the vehicle's efficiency, as measured by its lift-to-drag ratio, for the cruise segment.

This paper focuses on understanding the sensitivity of takeoff and landing distance to a series of aerodynamic and propulsive parameters of interest. In early stages of aircraft design, TOL performance analysis is often simplified down to correlating thrust-to-weight, wing loading, or other vehicle parameter ratios to TOL performance using historical aircraft data trends. Although this approach may produce adequate results for typical aircraft concepts, it is often insufficient for aircraft concepts that incorporate novel technologies and configurations. With the findings of this research, the goal is to identify potential benefits each parameter of interest can provide to the takeoff and landing distances of regional air mobility (RAM) aircraft [1, 2]. RAM aircraft, particularly those certified under the Normal Category [3], will be smaller than traditional commercial aircraft and will benefit more from increased electrification. Unlike larger aircraft, where electric systems contribute little to the overall thrust and have uncertain system-level benefits [4], RAM aircraft can be operated in an all-electric fashion, facilitating easy adoption of technologies like DEP [5].

III. Motivation

Electrification of the aircraft propulsion system is one of the key enablers of RAM aircraft. Electric aircraft are range-constrained due to the low specific energy of current battery technology [6]. This low specific energy means that optimizing battery-powered aircraft for energy efficiency is paramount, even more so than for fuel-powered aircraft. When sizing an aircraft, low-speed performance (i.e., takeoff and landing) dictates the wing size and the designer maximizes cruise efficiency as the geometry allows. DEP enables meeting the low-speed performance requirements with a wing area that is closer to the cruise optimum than for an aircraft without DEP [7]. Though the reduction in wing area leads to a reduction in viscous drag, DEP systems add viscous drag through podded propulsors. The net drag reduction is small, but the reduced wing area plays an important role in increasing utilization via faster cruise speed at equal lift-to-drag ratios.

To understand how much the wing area can be reduced due to DEP or another technology, one must have an accurate TOL model. An accurate TOL model is also necessary to determine from which airports RAM aircraft can operate. Estimating TOL distances requires low-speed aerodynamic data, a propulsion model that varies thrust with forward velocity, and other parameters to account for flight dynamics and power losses. Many of these factors are difficult to estimate during the early stages of conceptual design. For this reason, TOL analysis in conceptual design often relies on empirical methods or historical data. Although this approach may be adequate for aircraft concepts that are similar to historical aircraft designs, it is not appropriate for aircraft having novel designs or incorporating novel technologies.

The focus of this research is to understand what factors drive TOL distances via a sensitivity analysis for a RAM aircraft. Section IV describes how the work is performed, including input parameters and the mathematical approach. Section V quantifies the findings of the paper, including sensitivity analysis and TOL distances. The final sections summarize the work and describes future avenues of research.

IV. Methods

The equations of motion for takeoff and landing are well understood and easily programmed [8, 9]. The calculation begins at an initial time and integrates the net lift, weight, and net thrust, accounting for the thrust produced by the propellers and lost from drag, rolling resistance, and any other retardant forces. The Flight Optimization System (FLOPS) [10] performs TOL calculations with a fixed set of inputs divided across the airframe and propulsion systems. Many of the inputs can be assumed from historical values, though some are aircraft specific. The goal of this research is to understand how reactive TOL distance estimates are to variations in input factors. By knowing the impact each factor has on TOL estimates, a more informed decision can be made as to what effort is required to calculate the input factors

to determine TOL distances suitable for conceptual design. Of particular concern to this effort is the generation of low-speed aerodynamic information in the form of lift coefficient versus angle of attack (C_{L_α} curves) and drag polars (C_L-C_D curves).

A. Takeoff

The important distances for the calculation of takeoff performance are shown in Fig.1. Takeoff distance, for this study, is defined as the total distance from when the aircraft begins its ground roll until it clears a 50 ft obstacle. The distance from when the aircraft begins its ground roll until all its wheels lift off the ground is the takeoff roll distance. The distance at which the aircraft reaches its rotation speed and the pilot pulls back on the stick or yoke to pitch the vehicle's nose upwards is the rotation distance. Aircraft must also demonstrate adequate climb performance to an altitude of 1,000 ft in this study for the takeoff to be considered as a successful.

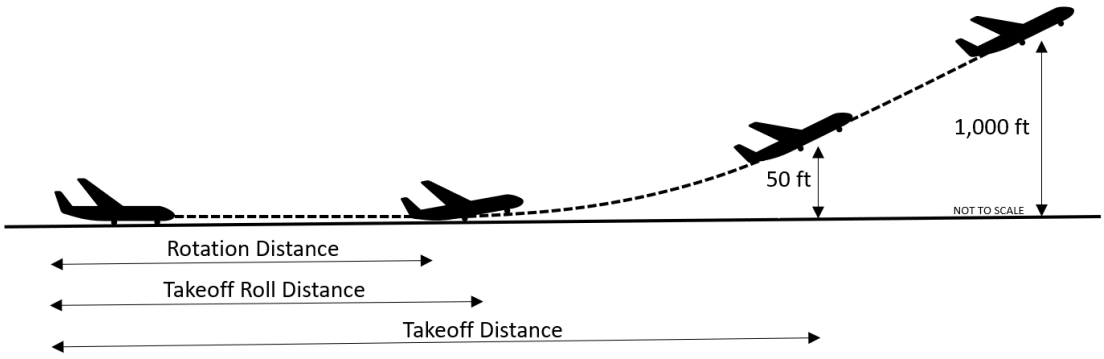

Fig. 1 Takeoff diagram.

The low-speed aerodynamic information for takeoff is built up using six parameters, three describing lift and three describing drag. These parameters are independent of the high-lift system utilized, making the approach suitable for DEP, traditional high-lift systems, or another lift augmentation technology. The lift parameters are: lift curve slope, C_{L_α}, maximum angle of attack, α_m, (which is limited by either stall or tail strike), and ΔC_L, an offset from the baseline curve that accounts for improvements in the high-lift system (which sets the lift coefficient at zero degree angle of attack). These improvements would typically come from either flaps/slats [11] and/or blown wings via DEP [7]. The wing incidence is used to adjust where on the C_{L_α} curve the aircraft begins its takeoff run. Figure 2 illustrates how adjustments to each of these parameters affect the baseline plots. Note that the inputs do not include the maximum lift coefficient, $C_{L_{\max}}$. Within this study, the $C_{L_{\max}}$ value is the point where the C_{L_α} curve becomes non-linear, as denoted by the start of the dashed line in Fig. 2. Though this is below the absolute peak $C_{L_{\max}}$, the difference leaves margin within the vehicle's operation. Approach is performed at 1.23 to 1.3 times stall speed, thus the vehicle is still within the linear region of the lift curve during approach as well.

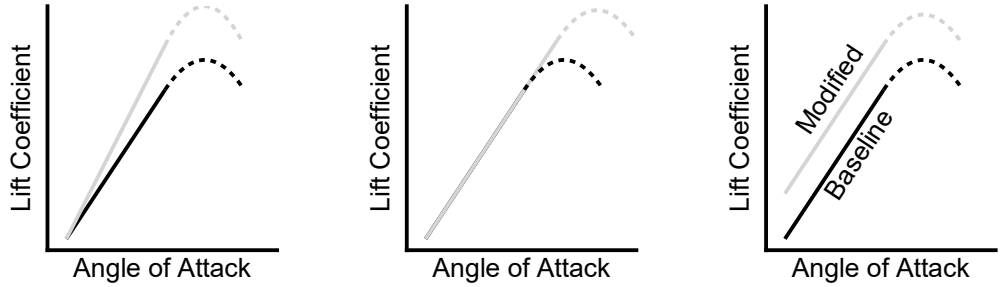

(a) Scaling factor on lift curve slope.

(b) Offset/delay in maximum angle of attack.

(c) Offset in lift coefficient for all angles of attack.

Fig. 2 Changes in the baseline lift curve plots due to variations in input parameters.

Drag polars take the form of a second-order polynomial with three coefficients, typified by Eq. (1). The first coefficient, k_2, is associated with lift induced drag through classic finite wing theory. The second coefficient is typically ignored in basic drag polars but is represented as k_1 in Eq. (1). The k_1 term is a result of asymmetry about the C_L=0 axis, which would result from wing camber due to either the airfoil or the flaps and slats. The final term is the lift-independent drag coefficient, better known as C_{D_0}. To understand the total effects of the drag polar on takeoff and landing performance estimates, the three coefficients in Eq. (1) will be varied in this study.

$$C_D = k_2 C_L^2 + k_1 C_L + C_{D_0} \tag{1}$$

Figure 3 shows how variations in the coefficients affect the drag polar. Notably, the k_2 term has a small impact on drag coefficient at the low lift coefficients —and correspondingly, low angles of attack— encountered during the majority of the takeoff run, as seen in Fig. 3a. Conversely, the k_1 term affects the drag coefficient at low lift coefficients more so than at high lift coefficients, as shown in Fig. 3b. Lastly, the C_{D_0} term directly shifts the drag polar left and right affecting all lift coefficients equally (see Fig. 3c).

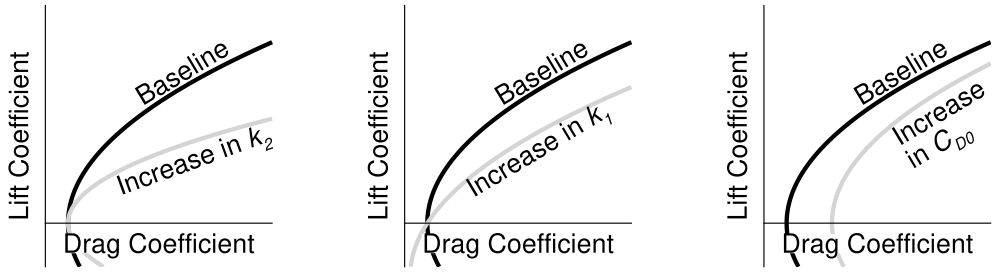

(a) Change in the non-linear term, k_2, in the drag equation.

(b) Change in the linear term, k_1, in the drag equation.

(c) Change in the zero-lift drag coefficient, C_{D0}.

Fig. 3 Changes in the drag polar due to variations in quadratic coefficients.

Future RAM aircraft are early candidates for adoption of electrified propulsion [5], so the parameters defining power are modeled as an electric motor in this study. During takeoff, the throttle setting is set to maximum power, and because electric motor power does not lapse with velocity, the motor power is constant from brake release to obstacle clearance. This requires imposing a minimum motor speed and maximum motor power as Fig. 4 shows. For this analysis, the maximum propeller speed is assumed to be more constraining than the maximum motor speed. Therefore, the maximum motor speed is not considered an independent constraint.

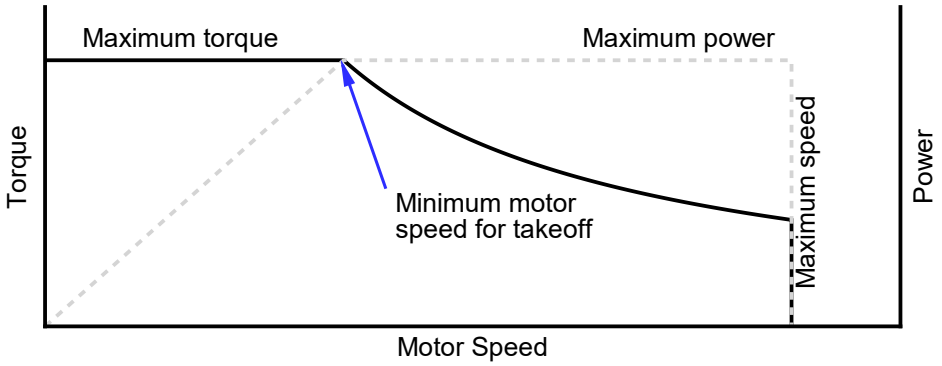

Fig. 4 Example electric motor map showing maximum torque and power conditions.

A propeller turns the motor's shaft power into thrust. The modeled propeller for this study is a variable pitch propeller, and the motor performance dictates the best RPM for a given forward velocity to optimize propeller efficiency, η_p. Detailed motor efficiency maps, like those created by McDonald [12], are not included in this analysis. Optimizing the motor-propeller system may lead to different operating points than optimizing the propeller performance alone. The

propeller model consists of two parts, a linear portion from advance ratios near zero to the linear breakpoint, J_L, where η_p depends on advance ratio, followed by a region of constant η_p. Figure 5 shows the model and key features. The Appendix shows how J_L is only a function of the maximum power and torque settings for the motor, thus the only input for the propeller is the maximum propeller efficiency. A third order polynomial, with coefficients determined via linear algebra, smoothly connects the sloped portion with the constant portion.

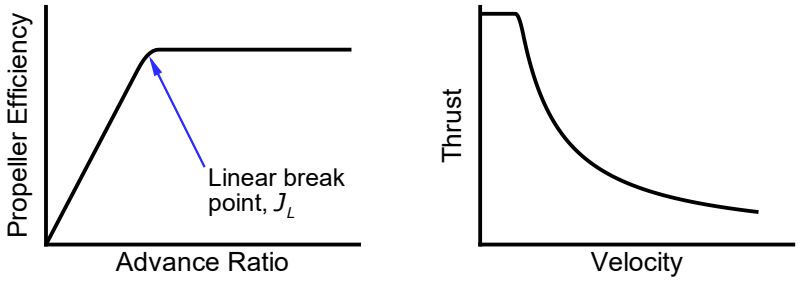

(a) Notional propeller efficiency. **(b) Notional thrust profile.**

Fig. 5 Idealized propeller efficiency and thrust profiles for a variable pitch propeller when the motor is set to maximum (takeoff) power.

Thrust is related to shaft power through Eq. (2), where T is thrust, P is shaft power, and V is forward velocity. Equation (2) becomes invalid at low speeds, and an additional model is required to develop a complete profile of thrust with velocity. Gudmundsson [13] provides a relation for static thrust based on propeller diameter and maximum power. This static thrust is held constant until J_L is reached. At advance ratios below J_L, the propeller efficiency increases with forward airspeed while the propeller-developed power drops with airspeed, resulting in constant thrust. When the advance ratio reaches J_L, the thrust will decrease with forward velocity per Eq. (2). Thus, knowing only the motor torque, motor power, and maximum propeller efficiency, we can build a simple model of the thrust at velocities from static to takeoff.

$$T = \frac{\eta_p P}{V} \tag{2}$$

B. Landing

Landing distance is defined as the distance from when the aircraft clears a 50 ft obstacle to when the vehicle comes to rest, and the landing roll distance is defined as the distance from when the wheels touch down to when the vehicle comes to rest (Fig.6). Nominally a three degree glideslope and flare comprise the airborne portion of the landing phase. Once the wheels touch down, braking is the dominant means of deceleration. Braking ability is initially limited by the weight on the wheels due to lift still being generated during the ground roll. The stall speed dictates the approach speed; for this analysis the approach speed is set to 130% of the stall speed. A lower stall speed would enable shorter landing distances.

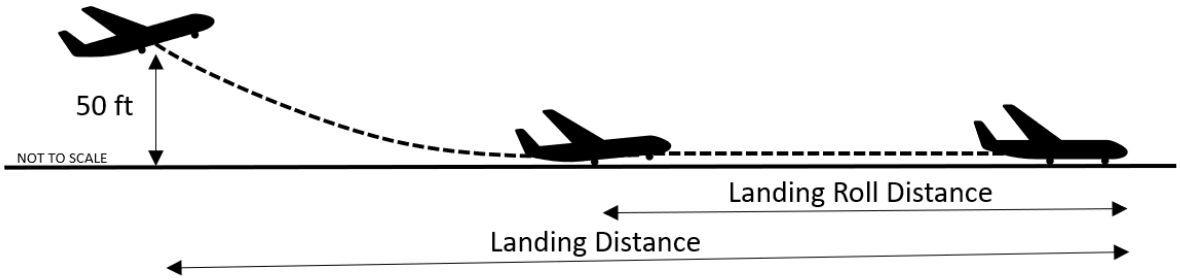

Fig. 6 Landing diagram.

The landing analysis uses a different lift curve and low-speed drag polar than the one developed for takeoff to account for the different high-lift system setting that is typically used during landing. The approach to building the landing lift curve and drag polar is the same as that described in Section IV.A, the main difference being adjustments to the values. The drag polar parameters (k_2, k_1, C_{D_0}) as well as the parameter setting the lift coefficient at zero degree angle of attack, ΔC_L, are adjusted to reflect possible lift augmentation in the landing setting of high-lift systems.

To model the landing distance, additional variables are required in addition to the drag polar characteristics. Variables such as the approach flight path, flare rate, sink rate at touchdown, and time after touchdown to apply the brakes will be further discussed in the FLOPS section below.

C. FLOPS

FLOPS is an aircraft sizing and synthesis tool [10] developed at NASA Langley Research Center beginning in the 1980s and continuously developed until 2011. FLOPS consists of six primary modules including weights, aerodynamics, propulsion, mission performance, takeoff and landing, and program control. For this study, the takeoff and landing module is the only module that is used. Aircraft and mission specific parameters are passed as inputs to FLOPS through a text-based file.

There are five additional parameters of interest that are varied for the FLOPS TOL simulations in this study. First is the wing incidence, defined in FLOPS as ALPRUN, which sets where along the lift curve the aircraft is during the ground run. The next two parameters are the rolling and braking friction coefficients, defined in FLOPS as ROLLMU and BRAKMU, respectively. The last two variables are landing specific: the approach angle and sink rate at touchdown, defined as APRANG and TDSINK in FLOPS. Some FLOPS input parameters are set directly by the ten variables discussed in Sections IV.A and IV.B above, such as the takeoff and landing drag polars themselves and the maximum angle of attack (α_m).

There are also FLOPS input parameters that are set indirectly by nine ten parameters discussed in Sections IV.A and IV.B (six to build the lift and drag polar curves and three to build the propulsion model). Among these are the maximum lift coefficient obtained using the maximum angle of attack and the lift curve, the minimum drag coefficient corresponding to the constant term in the drag polar, C_{D_0}, and a FLOPS engine deck using the propulsion model. The engine deck is built by scaling the thrusts at constant velocities with a power code scalar. The end result is thrust values at a range of specific power codes and forward velocities. Due to the assumption that the vehicle is electric, the fuel flow rate in the engine deck is set to a very low value (0.001 lb/hr) to simulate an electric vehicle's constant weight nature.

Multiple other FLOPS input parameters are set and kept constant for all simulations. The takeoff and landing altitude is set to sea level; thrust incidence is set to zero degrees signifying that the thrust and forward velocity vector of the aircraft are aligned; gear retraction is set to occur when the 50 ft obstacle is cleared; spoiler actuation is turned off due to our baseline aircraft not having spoilers and thus no spoiler effects are present; time after touchdown for brake application is set to four seconds; and the flare rate is set to four degrees per second. These latter two values, time to brake application and flare rate, are based on default values in FLOPS.

Each FLOPS TOL analysis goes through a series of tests to ensure that takeoff and landing was successful. The first test is to ensure that the aircraft has adequate climb performance to reach a 1,000 ft altitude (see Fig. 1). If the aircraft does not have the performance necessary to climb to 1,000 ft, the run is considered a failed climb case. For the landing calculations, FLOPS will sometimes report a warning that convergence for angle of attack was incomplete but will still continue with the landing analysis. This results in abnormal landing behavior and thus these cases are considered to have failed landing. The other failed landing case is when the FLOPS landing module does not produce a solution and returns a failed landing message. The same thing can occur with the takeoff analysis and thus those cases are considered to have failed takeoff. Ultimately, the successful cases include the configurations that are capable of climbing to 1,000 ft altitude and are successfully taking off and landing according to the FLOPS module.

D. Sensitivity Analysis Approach

To summarize Sections IV.A, IV.B, and IV.C, generating the aerodynamic model, comprising the C_L-α and drag polar curves, requires six inputs: lift curve slope, maximum angle of attack, lift coefficient at zero degree angle of attack, non-linear coefficient for the drag polar, linear coefficient for the drag polar, and the constant coefficient for the drag polar. Three factors comprise the propulsion system inputs: the maximum motor power, the static thrust coefficient, and the maximum propeller efficiency. FLOPS requires two more inputs for takeoff analysis: the average rolling coefficient of friction and the wing incidence. This results in eleven parameters of interest for takeoff. For landing there are three additional FLOPS inputs: the average braking coefficient of friction, the approach angle, and the sink rate at touchdown.

This results in fourteen parameter of interest for landing. Using FLOPS enables the exploration of a large sample space since it runs nearly instantly; still, a smart design of experiments is required as described below.

The sensitivity analysis is performed based on perturbing a known baseline case. For this study, a RAM-like aircraft based on the Cessna 402C was selected for the baseline case. Some baseline parameters are aircraft specific and were obtained by matching data available for the Cessna 402C. For the other parameters that are not aircraft specific, the values were obtained by selecting typical values. For the rolling and braking coefficients, values from MIL-STD-3013 for a dry runway were used [14]. The approach angle, three degrees, and sink rate, four feet per second, were both set to typical values for aircraft. Upper and lower bounds for most of the eleven takeoff input parameters and fourteen landing input parameters were found by perturbing the baseline value by twenty percent. For some parameters, the bounds were set using more appropriate values based on knowledge of typical variation for aircraft. The bounds for the takeoff and landing inputs can be seen in Table 1 and Table 2, respectively. The drag polar parameter values are not included in Table 1 nor in Table 2 since they are part of the proprietary data obtained from Cessna.

These bounds were used to create a Latin Hypercube design of experiments. This resulted in 10,000 distinct cases with values for each of the input parameters of interest that could then be passed to FLOPS to run the takeoff and landing analyses. Once the takeoff and landing information was calculated, a response surface model using a quadratic with interactions was fit to each of the two data sets to obtain a representation of the parameters of interest. A partial derivative was then taken of the response surface model with respect to each of the parameters of interest producing equations for the change in takeoff or landing distance with change in parameter of interest. The baseline values were then input into this equation to produce a sensitivity value that was then normalized by the baseline values and converted to a percentage. The end result is a sensitivity value for each parameter of interest that shows the percent change in takeoff or landing distance with a one percent change within the selected bounds of the parameter of interest. In order to ensure that the results were not bound specific, the study was also performed with bounds set at ten percent and forty percent change from the baseline values. Both of these produced results similar to those presented in Section V.

Table 1 Takeoff parameter bounds

Parameter	Lower Bound	Upper Bound
Lift Curve Slope (per degree)	0.0658	0.0987
Maximum Angle of Attack (degree)	12	16
C_L at Zero Degree Angle of Attack	0.3	0.6
Quadratic Term in the Drag Polar	-20%	+20%
Linear Term in the Drag Polar	-20%	+20%
Zero-Lift Drag Coefficient	-20%	+20%
Maximum Motor Power (HP)	260	390
Static Thrust Coefficient	0.4	0.6
Maximum Propeller Efficiency	0.56	0.84
Rolling Coefficient of Friction	0.016	0.024
Wing Incidence Angle (degree)	0	4

Table 2 Landing parameter bounds

Parameter	Lower Bound	Upper Bound
Lift Curve Slope (per degree)	0.0658	0.0987
Maximum Angle of Attack (degree)	12	16
C_L at Zero Degree Angle of Attack	0.3	1
Quadratic Term in the Drag Polar	-20%	+20%
Linear Term in the Drag Polar	-20%	+20%
Zero-Lift Drag Coefficient	-20%	+20%
Maximum Motor Power (HP)	260	390
Static Thrust Coefficient	0.4	0.6
Maximum Propeller Efficiency	0.56	0.84
Rolling Coefficient of Friction	0.016	0.024
Braking Coefficient of Friction	0.288	0.432
Approach Angle (degree)	2	4
Sink Rate at Touchdown (ft/s)	2	6
Wing Incidence Angle (degree)	0	4

V. Results and Discussion

The takeoff and landing distances were calculated as a function of change from the baseline specifications for the eleven takeoff parameters discussed in Section IV.A and fourteen landing parameters discussed in Section IV.B. The parameters of interest can be split into four groups: the propulsion group, which includes the static thrust coefficient, maximum motor power, and maximum propeller efficiency; the lift curve group, which includes the lift curve slope, maximum angle of attack, and the lift coefficient at zero degrees angle of attack; the drag polar group, which includes the quadratic and linear term in the drag polar as well as the zero-lift drag coefficient; and the FLOPS group, which includes the rolling friction coefficient and the wing incidence angle for takeoff and landing in addition to the braking friction coefficient, approach angle, and sink rate at touchdown for landing.

Figures 7 and 8 show the sensitivity of takeoff and landing distance to the input parameters. Bars that have a positive value indicate that an increase in that parameter leads to a longer takeoff or landing distance. Bars with a negative value indicate that an increase in that parameter leads to a reduction in takeoff or landing distance. For example, Fig. 7 shows the sensitivity to static thrust coefficient is negative; therefore, increasing the static thrust coefficient reduces takeoff distance, as is expected. Similarly, C_{D_0} has a positive value, meaning greater C_{D_0} values lead to longer takeoff distances.

A. Takeoff

To validate the takeoff analysis approach taken in this study, the RAM-like vehicle model was analyzed with all takeoff parameters at their baseline values. The takeoff distance was then compared to the actual takeoff distance of the reference vehicle using data obtained from Cessna. The result was a one percent difference between the two values. With the reference baseline model validated, the cases varying the eleven takeoff parameters were analyzed. A total of ten thousand cases were analyzed and the sensitivity analysis described in Section IV.D was performed. The result is the sensitivity tornado plot given in Fig. 7 that shows the percent change in takeoff distance from the baseline with an increase in the input parameter equal to one percent of the parameter's range (see Table 1).

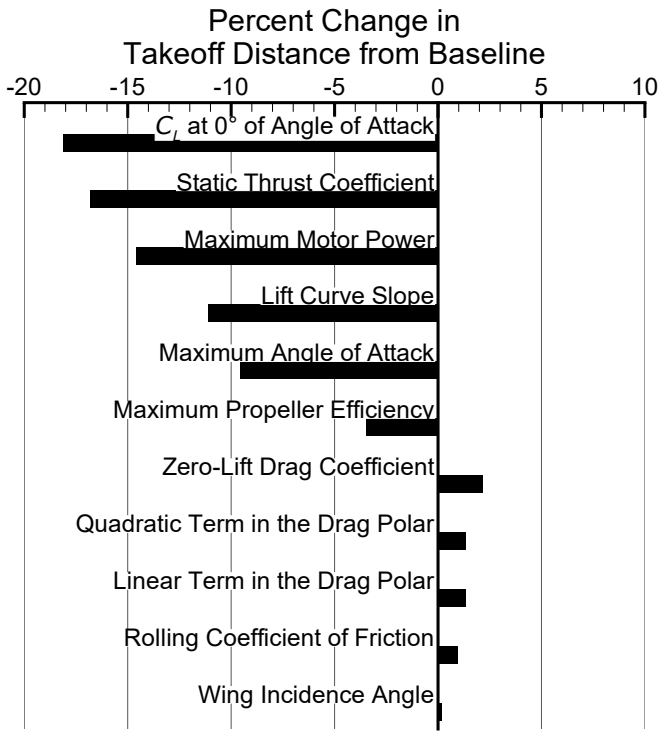

Fig. 7 Takeoff sensitivity tornado plot.

The FLOPS group contains the least impactful parameters for takeoff distance. The wing incidence angle is the least impactful of all the takeoff parameters. This can be attributed to the small drag penalty associated with an increase in the wing incidence. At low angles of attack, and thus low lift coefficients, the drag polar is still near its vertex and thus changes in lift coefficient result in small changes in drag coefficient. Rolling friction coefficient was also not very impactful. Although it physically contributes to the retardant force during the takeoff ground roll, it is small in magnitude compared to drag.

The drag polar parameters were of moderate importance to the takeoff distance. For the non-linear and linear terms, the modest effect they have on takeoff distance is due to the small drag polar changes associated with changes to these terms. The drag changes are especially small at low lift coefficients like those found throughout the takeoff roll. Although both of these parameters change the shape of the drag polar as shown in Fig. 3, neither of them does so enough within the bounds selected to be a main driver of takeoff distance. The zero-lift drag coefficient is the most impactful of the three parameters due to it directly shifting the drag polar and affecting the low lift coefficient portion of the drag polar. The low-speed drag polar parameters have a moderate effect on takeoff distance but are not nearly as impactful as the propulsion or lift curve slope parameters.

The lift curve parameters were some of the most impactful for takeoff distance. The maximum angle of attack defines the upper limit for the lift coefficient that can be obtained by the aircraft. By being able to obtain a higher angle of attack, a higher lift coefficient can be obtained increasing the lift that can be generated and thus the aircraft can climb to the 50 ft obstacle clearance height in a shorter distance. With a higher lift coefficient, the aircraft also requires a lower speed to lift off during the ground roll. The aircraft will take a shorter time to accelerate to this lower lift off speed shortening the takeoff distance. Maximum angle of attack is not the only parameter that defines the upper limit of lift; the lift curve slope and lift coefficient at zero degrees angle of attack also contribute vastly to defining the max lift. These three parameters have their largest effects after the rotation speed is obtained. Rotation speed defines the point at which the aircraft may begin to rotate and generate additional lift to take off. It is during and after this rotation when these three parameters become important factors. Increasing any of these three parameters will result in an increase in lift which will decrease the time to rotate and climb to 50 ft. The time saved may seem small in magnitude, but this is all occurring at a relatively high speed. Thus any time reduction in these phases can decrease takeoff distances significantly as shown in Fig. 7. Both lift coefficient at zero degrees angle of attack and lift curve slope determine

the amount of lift generated during the takeoff roll. The higher the lift generated during the takeoff roll, the lower the change in lift has to be during rotation to obtain liftoff, saving time and ultimately leading to shorter takeoff distances. Another effect, although not as impactful, is that with higher lift during the takeoff roll there is less weight on wheels and thus less rolling resistance. These effects during the ground roll are much stronger for lift coefficient at zero degree angle of attack compared to lift curve slope since the ground roll happens at low angles of attack where an increase in lift coefficient is much larger due to a shift upwards in the lift curve than an increase in its slope. These compounding effects are why lift coefficient at zero degrees angle of attack ends up being more impactful than the lift curve slope and both of these end up being more impactful than maximum angle of attack.

The propulsion group is the final group and it includes parameters that are quite impactful to takeoff distance. This is due to the fact that the propulsion system is responsible for accelerating the vehicle to the specific and required V-speeds. The static thrust coefficient is the most impactful as it is a scalar of the net thrust being generated by the aircraft within the constant thrust range which occurs until J_L is reached. The maximum motor power also affects the thrust generated notably, but thrust lapses with velocity as shown by Eq. (8) and thus maximum motor power is slightly less impactful than the static thrust coefficient. The propeller efficiency has a much smaller impact on takeoff as an increase in efficiency only leads to a small increase in net thrust. The effects of the propulsion group parameters can be reduced to a kinematics problem, the greater the propulsion force the quicker the vehicle can accelerate and reach the required speed needed to takeoff.

B. Landing

The RAM-like vehicle landing model was validated by comparing its results to the actual landing performance of the reference vehicle using data obtained from Cessna. The result was a half a percent difference in landing distance. The same sensitivity analysis performed for takeoff was done for landing and the result is the sensitivity tornado plot given in Fig. 8.

Unlike takeoff where the parameters in the propulsion group were among the most impactful, for landing these parameters have almost no impact. This is due to the low use of the propulsion system by the aircraft during landing.

The FLOPS group includes both parameters that are impactful and parameters that have little effect on landing distance. The rolling coefficient of friction has a small effect on landing distance because only a small portion of the landing roll is performed without braking. The sink rate at touchdown is also of little importance to landing since as long as the aircraft touches down and is capable of braking, the model is indifferent as to the vertical rate of the aircraft within the range selected shown in Table 2. On the other hand, parameters such as wing incidence have a large effect on landing distance. The impact of this parameter is primarily due to the weight on wheels effect during the landing roll. The higher the wing incidence, the higher the lift generated during the landing roll. Greater lift during the landing roll means less weight on wheels, lowering the braking ability of the vehicle. Braking ability is crucial as it is the main form of deceleration for the aircraft, and, therefore, braking coefficient is one of the most impactful parameters for landing distance. Lastly, the approach angle is the most impactful parameter in this group because the landing distance is measured from the 50 ft obstacle point. Thus, if the approach angle is steeper, it will enable the vehicle to touch down quicker, decreasing the landing distance.

The lift curve group includes two of the most impactful parameters for landing, which are the maximum angle of attack and the lift curve slope. Just like with takeoff, this is due to the obtainable lift coefficient limit that these parameters impose. In landing, a higher lift coefficient implies a lower a lower approach speed and thus a lower touchdown speed. With this lower speed at touchdown, the aircraft will need less distance to decelerate to a stop ultimately decreasing the landing distance. Although this lift coefficient limit is highly impactful, the effect of lift generation during the ground roll reduces the importance of lift curve slope and lift coefficient at zero degrees angle of attack due to the previously explained decrease in braking ability. For this reason lift curve slope and especially lift coefficient at zero degrees angle of attack are less impactful compared to takeoff, where the weight on wheels effect was additive with the lift coefficient limit.

The drag polar parameters are grouped together in the middle of Fig. 8. The zero-lift drag coefficient was the most impactful of the three. Like with takeoff, this is due to the zero-lift drag coefficient affecting the drag polar the most at low lift coefficients where the landing roll occurs. The larger drag coefficients increase the drag of the vehicle contributing to a higher deceleration of the aircraft and shorter landing distances. Although the non-linear and linear terms also offer this benefit, it is much smaller in magnitude due to the vertex effect of quadratics.

The trends and sensitivities in this study are solely for a RAM-sized aircraft, specifically for a Cessna 402C-like vehicle. The results may change for vehicles with higher or lower thrust-to-weight ratios or vehicles using high-lift

technologies that alter the vehicle's performance in ways not captured in this study. Vehicles with high thrust-to-weight ratios will accelerate faster, spending less time and distance at low-speeds, enabling successful takeoff with lower performing aerodynamics.

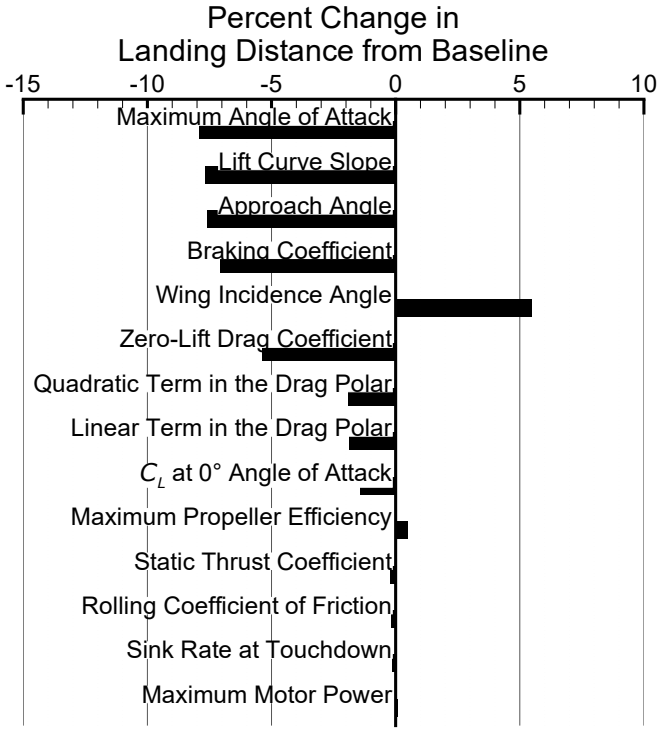

Fig. 8 Landing sensitivity tornado plot.

VI. Concluding Remarks

Takeoff and landing is a crucial part of any aircraft mission and understanding how parameters affect the calculation of TOL performance is important to obtain a feasible and optimal conceptual design. In this study it was found that for takeoff, the most impactful parameters are those relating to propulsion and the lift curve, all parameters that can be estimated using conceptual level fidelity tools. The drag polar parameters are moderately impactful but not near the level of the most impactful parameters. For landing, once again, the lift-curve parameters are some of the most impactful parameters, as well as the approach angle, the wing incidence, and the braking coefficient. These last three parameters are often overlooked by many empirical approaches to estimate TOL performance. For landing, like for takeoff, the drag polar parameters were amongst the moderate impactful parameters. The drag polar parameters in both cases had an effect but were not main drivers of TOL performance.

VII. Future Work

This research focused on determining the effect and sensitivity of various parameters on takeoff and landing distance estimations. The next step is to execute high-lift trades while sizing a RAM aircraft to measure how the wing sizing impacts cruise efficiency and overall vehicle utilization. Going from aerodynamic performance to geometry is an inverse design problem, and some high-lift performance capabilities may be unobtainable. An aspect of the sizing work is to learn how to practically develop wing geometries and DEP systems that generate the aerodynamic characteristics identified in this work.

Another future enhancement is to generate a propulsion model incorporating more facets of the system, including motor efficiency performance, battery performance estimations, and a means of relating DEP lift generation to thrust generation. Having a design theory to understand how to size DEP systems to meet a variety of performance goals

would aid in the technology's adoption.

Appendix

The following steps demonstrate that the break point in advance ratio, J_L, where propeller efficiency, η_p, becomes constant is only a function of motor torque and power. If η_p starts at zero with zero airspeed and climbs linearly to $\eta_{p,max}$ at J_L, then within this range

$$\eta_p = \frac{J}{J_L}\eta_{p,max} \tag{3}$$

$$J = \frac{V}{nD} \tag{4}$$

where n is the rotational speed in revolutions per second and D is the propeller diameter. Equation (5) defines the motor speed with the minimum motor speed, ω_{min}, set by the maximum motor torque and power.

$$\omega_{min} = \frac{P}{Q} \tag{5}$$

Knowing that $n = \omega/2\pi$ and substituting Eq. (5) into Eqs. (3) and (4) generates Eqs. (6) and (7). Equation (8), repeated from Eq. (2) in the main body of this text, relates a propeller's thrust to its power at "high" velocities.

$$\eta_p = \frac{2\pi V Q \eta_{p,max}}{J_L P D} \tag{6}$$

$$J = \frac{2\pi V Q \eta_{p,max}}{P D} \tag{7}$$

$$T = \frac{\eta_p P}{V} \tag{8}$$

Substituting η_p from Eq. (6) into Eq. (8), the equation for thrust becomes Eq. (9).

$$T = \frac{2\pi Q \eta_{p,max}}{J_L D} \tag{9}$$

Equation (9) shows within this linear range, thrust does not vary with forward velocity, thus $T = T_s$, which is known. The one unknown within Eq. (9) is J_L, thus we can solve for its value. This also shows that increasing motor torque decreases the minimum motor speed to achieve maximum power, which leads to higher flight velocities before maximum propeller efficiency can be achieved. In this model, a lower torque motor spinning with a higher speed would be superior to a high torque motor that operates at a lower speed.

VIII. Acknowledgments

This work was funded by NASA's Convergent Aeronautics Solution Project of the Transformative Aeronautics Concepts Program under NASA's Aeronautics Research Mission Directorate. The authors thank NASA for their support of this research.

References

[1] Borer, N. K., Patterson, M. D., and Blaesser, N. J., "Regulatory Considerations for Future Regional Air Mobility Aircraft," NASA Technical Memorandum NASA/TM-2023-0006666, NASA, May 2023. URL https://ntrs.nasa.gov/citations/20230006666.

[2] Antcliff, K., et al., "Regional Air Mobility: Leveraging Our National Investments to Energize the American Travel Experience," NASA Technical Memorandum NASA/TM-2023-0014033, NASA, Apr. 2021. URL https://ntrs.nasa.gov/citations/20210014033.

[3] "Part 23 — Airworthiness Standards: Normal Category Airplanes," https://www.ecfr.gov/current/title-14/chapter-I/subchapter-C/part-23, Accessed: Feb 2024.

[4] Marien, T., Blaesser, N. J., Guynn, M. D., Kirk, J., Frederick, Z. J., Fisher, K., Schnieder, S., Thacker, R., and Frederic, P., "Results for an Electrified Aircraft Propulsion Design Exploration," AIAA Paper 2021-3280, Aug. 2021. https://doi.org/10.2514/6.2021-3280.

[5] Stoll, A. M., and Mikic, G. V., "Design Studies of Thin-Haul Commuter Aircraft with Distributed Electric Propulsion," AIAA Paper 2016-3765, 2016. https://doi.org/10.2514/6.2016-3765.

[6] McDonald, R. A., "Establishing Mission Requirements Based on Consideration of Aircraft Operations," *AIAA Journal*, Vol. 50, No. 3, 2013. https://doi.org/10.2514/1.C031878.

[7] Borer, N. K., Patterson, M. D., Viken, J. K., Moore, M. D., Bevirt, J., Stoll, A. M., and Gibson, A. R., "Design and Performance of the NASA SCEPTOR Distributed Electric Propulsion Flight Demonstrator," AIAA Paper 2016-3920, June 2016. https://doi.org/10.2514/6.2016-3920.

[8] Roskam, J., and Lan, C. T. E., *Airplane Aerodynamics and Performance*, Darcorporation, Lawrence, 2016.

[9] Hurt, H. H., *Aerodynamics for Naval Aviators*, Naval Air Systems Command United States Navy, Renton, 1965.

[10] McCullers, L. A., "Aircraft Configuration Optimization Including Optimized Flight Profiles," *Recent Experiences in Multidisciplinary Analysis and Optimization*, edited by J. Sobieski, NASA CP 2327 Pt.1, 1984, pp. 395–413.

[11] van Dam, C., "The Aerodynamic Design of Multi-Element High-Lift Systems for Transport Airplanes," *Progress in Aerospace Sciences*, Vol. 38, 2002, pp. 101–144.

[12] McDonald, R. A., "Electric Propulsion Modeling for Conceptual Aircraft Design," AIAA Paper 2014-0536, Jan. 2014. https://doi.org/10.2514/6.2014-0536.

[13] Gudmundsson, S., *General Aviation Aircraft Design*, 2nd ed., Butterworth-Heinemann, Oxford, UK, 2021.

[14] MIL-STD-3013, "GLOSSARY OF DEFINITIONS, GROUND RULES AND MISSION PROFILES TO DEFINE AIR VEHICLE PERFORMANCE CAPABILITY," , 2003.